ORIGINAL ARTICLE

Efficacy of combined icotinib and pemetrexed in *EGFR* mutant lung adenocarcinoma cell line xenografts

Jiadong Cui[1,2], Yan Zhang[3], Di Su[2], Tao Li[1] & Yu Li[1] (iD)

1 Department of Respiratory Medicine, Qilu Hospital of Shandong University, Jinan, China
2 Department of Respiratory Medicine, Dong'e County People's Hospital, Liaocheng, China
3 Department of Respiratory Medicine, Jinan No. 4 People's Hospital, Jinan, China

Abstract

Background: The combination of *EGFR* tyrosine kinase inhibitors (TKIs) and chemotherapy is thought to increase treatment efficacy in non-small-cell lung cancer (NSCLC). This study investigated the efficacy and potential mechanisms of different combined modes of icotinib plus pemetrexed in *EGFR*-mutant lung adenocarcinoma cell line xenograft models.

Methods: Nude mice were subcutaneously injected with *EGFR*-mutant human lung adenocarcinoma cells (HCC827) and randomized into six treatment groups. Tumor xenograft volumes were monitored and recorded. Microvessel density (MVD) and proliferation and apoptosis rates were evaluated with CD34 positive cell counting, and Ki-67 and caspase-3 scores, respectively, and determined via immunohistochemistry. Thymidylate synthase (TS), *EGFR*, and downstream signaling molecule expression was detected by Western blotting.

Results: The volume and weight of tumor xenografts in the sequential pemetrexed followed by icotinib (Pem-Ico) group and the concurrent icotinib and pemetrexed (Ico + Pem) group were significantly smaller than those in the control, pemetrexed (Pem), icotinib (Ico), and sequential icotinib followed by pemetrexed (Ico-Pem) groups. Compared to other groups, a decrease in the MVD and proliferation rate and an increase in the apoptosis rate were observed in the Pem-Ico and Ico + Pem groups. TS expression and *EGFR*, AKT, and MAPK phosphorylation were significantly reduced in the Pem-Ico or Ico + Pem groups.

Conclusions: Pem-Ico had additive antitumor activity in vivo, similar to Ico + Pem, both of which are suggested as potentially optimized strategies for treating *EGFR*-mutant lung adenocarcinoma.

Introduction

Lung cancer is the leading cause of death of all cancer types worldwide.[1] Approximately 80–85% of lung cancers are non-small-cell lung cancer (NSCLC), and more than half of the patients diagnosed with NSCLC are in advanced stages of disease. Lung adenocarcinoma is the most common histological subtype of NSCLC and accounts for more than 50% of all NSCLC cases.[2] Systemic treatment plays a central role in clinical management. Platinum-based chemotherapy affords a median survival of approximately 8–10 months.[3] Currently, the development of agents that

target *EGFR* mutation and *ALK* rearrangement have provided a class of novel targeted therapeutic agents.[4,5] EGFR-tyrosine kinase inhibitors (TKIs) provide a clear clinical benefit compared to platinum-based chemotherapy in patients with advanced *EGFR*-mutant NSCLC,[6] and are now standard first-line therapy for patients with activating *EGFR* mutations. However, acquired EGFR-TKI resistance and disease progression eventually occurs in most of these patients after a median of 10–14 months.[7]

Given the different mechanisms of chemotherapy and target agents, combination treatment with chemotherapy

and EGFR-TKIs might further increase the survival benefit in advanced NSCLC patients. However, four phase III studies did not show a clinical benefit of concurrent combinations in unselected patients.[8–11] Two primary reasons proposed for these failures are that potential antagonistic effects of EGFR-TKIs and chemotherapy existed in the concurrent combination and that patients with wild-type *EGFR* were enrolled in the studies. The phase III FASTACT-2 study conducted in unselected patients with advanced NSCLC indicated that intercalated combinations of chemotherapy and EGFR-TKIs significantly improved progression-free survival (PFS) and overall survival (OS), with no differences in toxicity observed compared to chemotherapy plus placebo, and treatment benefits were only observed in patients with activating *EGFR* mutations.[12] However, this study did not address if the combination treatment was more effective than EGFR-TKI monotherapy in patients with activating *EGFR* mutations.

Pemetrexed, as an inhibitor of thymidylate synthase (TS), dihydrofolate reductase (DHFR), and glycinamide ribonucleotide formyltransferase (GARFT), arrests tumor cells primarily in the S phase and induces apoptosis in a broad spectrum of solid tumors, including NSCLC.[13] Pemetrexed is widely used for the treatment of non-squamous NSCLC patients, with a definite curative effect and less toxicity.[14] A preclinical study showed that cytotoxic synergism was observed when TKI-sensitive human NSCLC cell lines were exposed to concurrent pemetrexed and erlotinib or sequential pemetrexed followed by erlotinib.[15] Another in vitro experiment by Feng *et al.* demonstrated that the synergistic effect on *EGFR*-mutant lung adenocarcinoma cell lines was only observed with the sequential administration of pemetrexed followed by icotinib/erlotinib.[16] However, Chen *et al.* reported that concurrent pemetrexed and gefitinib improved PFS compared with gefitinib alone in advanced non-squamous NSCLC patients with activating *EGFR* mutations.[17] Although these results suggest a potential benefit from the combination of pemetrexed and EGFR-TKIs in NSCLC with activating *EGFR* mutations, the optimal administration schedule needs to be elucidated.

Icotinib is a specific and effective EGFR-TKI with a relatively short elimination half-life that has exhibited a positive clinical anti-tumor effect in advanced NSCLC patients and fewer drug-related adverse events than gefitinib.[18] As a critical step for the initial development and progression of solid tumors, angiogenesis is understood to be an important therapeutic target.[19] Activation of the *EGFR* pathway is involved in angiogenesis, as well as cell proliferation and anti-apoptosis, and these processes are affected by *EGFR* inhibition.[20] A previous in vitro study reported that enhanced anti-vascular endothelial growth factor activity in NSCLC cell lines was observed under the sequence of

paclitaxel followed by gefitinib, instead of the opposite sequence.[21] Microvessel density (MVD), which reflects the formation of new vessels, is often used as an effective marker for assessing angiogenesis.[22] Therefore, we hypothesize that the combination of icotinib and pemetrexed may produce schedule-dependent effects of reducing MVD in vivo.

The aim of this study was to explore the efficacy and potential mechanisms of different combined schedules of icotinib and pemetrexed in *EGFR*-mutant lung adenocarcinoma cell line (HCC827) xenograft models, which may provide potentially beneficial treatment strategies.

Methods

Cell line and culture

Non-small cell lung cancer cell line HCC827 cells bearing an activating deletion mutation in exon 19 (19del) were obtained from the Shanghai Cellular Library, Chinese Academy of Medical Sciences. Cells were grown in RPMI-1640 (HyClone, Shanghai, China) medium supplemented with 10% fetal bovine serum (Gibco, Grand Island, NY, USA) and 1% penicillin/streptomycin (100 units/mL penicillin and 100 μg/mL streptomycin, HyClone). All cells were incubated in a humidified incubator containing 5% CO_2 at 37°C.

Drugs

Icotinib and pemetrexed were purchased from Beta Pharma Inc. (Hangzhou, China) and Qilu Pharmaceuticals (Jinan, China), respectively.

Establishment of nude mice xenograft models, treatment strategies

Four to six-week old female Balb/c-nu athymic mice purchased from the Nanjing Biomedical Research Institute of Nanjing University were fed freely in a specific pathogen-free (SPF) environment with 12-hour light/dark. The research protocol was approved, and all of the animal experiments were performed in accordance with the Institutional Guidelines of the Shandong University Animal Care and Use Committee. Mice were injected subcutaneously in the axillary region with 5×10^6 HCC827 cells that had been diluted in 200 μL of RPMI-1640 without fetal bovine serum.

When tumors reached a mean volume of 150 mm^3, the mice were randomized into six groups (six mice/group). The treatment plans for each of the groups were as follows. Icotinib (Ico) group: icotinib was prepared by dissolving in 0.5% sodium carboxymethyl cellulose and was later orally

administered to the mice at a dose of 60 mg/kg daily from days 1 to 5, five times per week. Pemetrexed (Pem) group: pemetrexed was first diluted in normal saline and then administered intraperitoneally at a dose of 250 mg/kg once a week. Dosages of icotinib and pemetrexed were based on previous related animal experiments.[23,24] Sequential pemetrexed followed by icotinib (Pem-Ico) group: pemetrexed was administered on day 1 and then icotinib was from days 2 to 6; both pemetrexed and icotinib were used at the same dosage as in the single drug groups. The same drug dosages were also applied to the other parallel groups. Sequential icotinib followed by pemetrexed (Ico-Pem) group: icotinib was administered from days 1 to 5 and then pemetrexed on day 6. Concurrent icotinib and pemetrexed (Ico + Pem) group: icotinib was administered from days 1 to 5 and concurrent pemetrexed on day 1. The control group (Control): 0.5% sodium carboxymethyl cellulose was administered at a dose of 0.01 mL/g daily, five days a week. All treatments were administered for a total of three weeks. The body weights and tumor volumes of the mice were monitored every three days. The tumor volume was calculated by the ellipsoid formula with an expression of 3.142 (larger diameter × [smaller diameter]^2)/6.[25] The growth-curves of the tumor volume were then drawn according to time in all groups.

The mice were sacrificed by cervical dislocation at the end of the 21st day. The tumor xenografts were collected by dissection and subsequently weighed. The tumor growth inhibition rate (TGIR) was assessed using the formula: (1-mean tumor weight of the treatment group/mean tumor weight of the control group) × 100%.[23] Half of the tumors were fixed with 4% neutral formaldehyde and embedded in paraffin, while the other half were refrigerated at −80°C for subsequent experiments.

Histopathological observation and immunohistochemistry

Serial tissue sections (4 μm thick) from tumors wrapped with paraffin were processed for hematoxylin and eosin (H&E) and immunohistochemical staining. The tissue sections were immunostained by anti-CD34, anti-Ki-67, and anti-caspase-3 according to the manufacturer's instructions (Servicebio, Wuhan, China). Two independent pathologists blinded to the study assessed the results of H&E and immunohistochemical staining. CD34 was mainly expressed in the cytoplasm and membrane of vascular endothelial cells. MVD was measured by counting the number of cells that expressed CD34 in each xenograft tumor tissue. The highly vascular areas were found by scanning sections at low power (10 × 10), and then a vessel count was performed on a × 200 field with the reference that one brown stained endothelial cell counted as a vessel.

After assessing the vessel counts in five fields, the mean number was selected as MVD. The proliferation and apoptosis rates were assessed by Ki-67 and caspase-3 scores and expressed as the percentage of positive cells among all tumor cells. Five fields were randomly examined per section, and approximately 100 cells were observed per field at high power (10 × 40).

Western blotting

The total protein in tumor tissues was extracted from each group and the protein concentration was determined (BCA Protein Assay Kit, CWBIO, Beijing China) following the manufacturer's instructions. Thereafter, loading buffer was added into the extracted protein samples to boil for 10 minutes at 95°C. The total proteins of each group were electrophoretically separated with 10% sodium dodecyl sulfate–polyacrylamide gel electrophoresis (SDS-PAGE) gels and then transferred onto polyvinylidene difluoride membranes (Millipore, Billerica, MA, USA). After blocking with 5% bovine serum albumin at room temperature for one hour, primary antibodies including anti-TS, anti-EGFR, anti-phospho-EGFR, anti-AKT, anti-phospho-AKT, anti-MAPK, anti-phospho-MAPK, and anti-β-actin antibody (Abcam, Cambridge, MA, USA) were added overnight and incubated at 4°C. The membranes were washed three times the next day with tris-buffered saline and tween-20 before adding horseradish peroxidase-conjugated secondary antibody (Proteintech Group Inc., Rosemont, IL, USA). Immunoreactive protein bands were visualized using the enhanced chemiluminescence (ECL) system (Pierce, Rockford, IL, USA) and were developed using the Western Blot Imaging System (Cell Biosciences, Santa Clara, CA, USA). The density of each band was measured using ImageJ software (NIH, Bethesda, MD, USA).

Statistical analysis

All collected data were expressed as the mean ± standard deviation. Statistical analysis was performed by one-way analysis of variance (multiple group comparisons) or T test (pairwise comparison) using SPSS version 22.0 (IBM Corp., Armonk, NY, USA). $P < 0.05$ was considered to be significant.

Results

Growth impact of combined treatment with icotinib and pemetrexed

The effects of the combination of icotinib and pemetrexed on *EGFR*-mutant lung adenocarcinoma tumor growth were investigated using HCC827 cell line xenograft models. The

tumor xenograft volumes of the control group gradually increased, while tumor xenograft growth in the Pem, Ico, and Ico-Pem groups slowed. In contrast, decreased tumor volumes were observed in the Pem-Ico and Ico + Pem groups. At the end of the 21st day, the tumor volumes in the Pem-Ico (62.38 ± 30.23 mm^3) and Ico + Pem (73.69 ± 30.73 mm^3) groups were significantly smaller than those of the control (689.12 ± 253.43 mm^3), Pem (393.64 ± 154.73 mm^3), Ico (236.56 ± 121.95 mm^3), and Ico-Pem (149.33 ± 65.11 mm^3) ($P < 0.05$) groups. The tumor volumes of the Ico and the Ico-Pem groups were smaller than those of the Pem group ($P < 0.05$), while the tumor volumes of the Pem group were smaller than those of the control ($P < 0.05$). However, there were no significant differences between the Pem-Ico and Ico + Pem groups or the Ico and Ico-Pem groups ($P > 0.05$) (Fig 1).

Effect on tumor weight and growth inhibition rate after combined treatment with icotinib and pemetrexed

The tumor weights of the five treatment groups were reduced when compared to those of the control group ($P < 0.05$). The tumor weights of the Pem-Ico and the Ico + Pem groups were significantly lower than the Pem, Ico, and Ico-Pem groups ($P < 0.05$). The TGIR among the five treatment groups in ascending order were: Pem, Ico, Ico-Pem, Ico + Pem, and Pem-Ico (Table 1).

Drug-related adverse events

Adverse reactions were measured by monitoring the effects of the treatments on mouse weight. Changes in the body weight of nude mice before and after treatment were not

significant ($P > 0.05$) (Table 2). The behavior of nude mice was not significantly affected during the experiment.

Histological morphology influence of combined treatment with icotinib and pemetrexed

Routine H&E stained slides of tumor xenografts were examined under an optical microscope. Visible tumor tissue with a solid structure was observed. The tumor cells separated by fibrous tissue into various nests showed fusiform or elliptic form, obvious nucleolus, and were different sizes. After treatment, the contents of the tumor cells were reduced and the fibrous tissue increased among the five drug treatment groups, particularly in the Pem-Ico and Ico + Pem groups (Fig 2).

Microvessel density impact of combined treatment with icotinib and pemetrexed

The MVD among the six groups was significantly different (F = 86.49; $P < 0.05$). First, the MVDs in the Ico (25.62 ± 2.35), Pem-Ico (18.02 ± 2.94), Ico + Pem (19.93 ± 2.14), and the Ico-Pem (26.72 ± 2.32) groups were significantly lower than the control (39.38 ± 1.49) and Pem groups (36.85 ± 2.29) ($P < 0.01$). Furthermore, the Pem-Ico and Ico + Pem group values were significantly lower than those of the Ico and Ico-Pem groups ($P < 0.01$). However, the MVD between the three paired groups (Pem-Ico vs. Ico + Pem, Ico vs. Ico-Pem, and Pem vs. the control) were not significantly different ($P > 0.05$). These findings showed the additive effect of MVD inhibition in sequential pemetrexed followed by icotinib and concurrent icotinib combined with pemetrexed treatment (Fig 3).
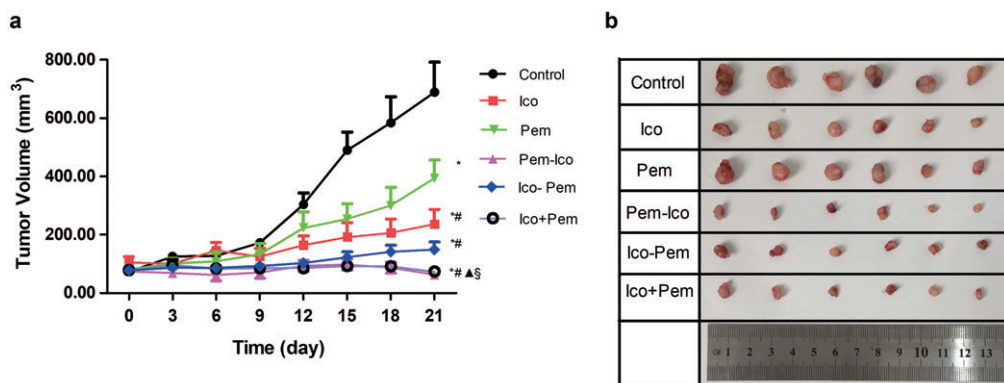
Figure 1 Effects of different combinations of icotinib (Ico) and pemetrexed (Pem) on tumor xenograft growth and tumor size. Nude mice bearing lung adenocarcinoma HCC827 cell xenograft tumors received different treatments for three weeks when the mean tumor volume reached 150 mm^3 (n = 6 mice/group). Groups: control; Ico; Ico-Pem, sequential Ico followed by Pem; Ico + Pem, concurrent Ico and Pem; Pem; Pem-Ico, sequential Pem followed by Ico. (**a**) Tumor growth curves of each group. $P < 0.05$ versus *control, #Pem, ▲Ico, §Ico-Pem. (**b**) Tumor sizes at the end of the 21st day.

Table 1 Tumor weight (mean $\pm$ SD) and proliferation inhibition rate at the end of the 21st day ($n = 6$ mice/group)

Group	3-week Icotinib	3-week Pemetrexed	Tumor weight (g)	TGIR%
Control	Vehicle	Vehicle	0.41 $\pm$ 0.16	0.0
Ico	60 mg/kg d1-d5	—	0.13 $\pm$ 0.06†,‡	68.3
Pem	—	250 mg/kg d1	0.24 $\pm$ 0.15†	41.5
Pem-Ico	60 mg/kg d2-d6	250 mg/kg d1	0.05 $\pm$ 0.03†,‡,§,¶	87.8
Ico-Pem	60 mg/kg d1-d5	250 mg/kg d6	0.11 $\pm$ 0.04†,‡	73.2
Ico + Pem	60 mg/kg d1-d5	250 mg/kg d1	0.06 $\pm$ 0.02†,‡,§,¶	85.4

$P < 0.05$ versus. †Control, ‡Pemetrexed (Pem), §Icotinib (Ico), and ¶Ico-Pem. Ico-Pem, sequential Ico followed by Pem; Ico + Pem, concurrent Ico combined with Pem; Pem-Ico, sequential Pem followed by Ico; SD, standard deviation; TGIR, tumor growth inhibition rate.

Table 2 Body weight of the nude mice before and after treatments ($n = 6$ mice/group, mean $\pm$ SD)

Group	Initial body weight (g)	Final body weight (g)
Control	21.75 $\pm$ 0.90	22.87 $\pm$ 1.17†,‡
Ico	21.20 $\pm$ 0.85	22.42 $\pm$ 1.24†,‡
Pem	20.47 $\pm$ 0.85	21.47 $\pm$ 0.95†,‡
Pem-Ico	20.37 $\pm$ 0.91	21.32 $\pm$ 0.62†,‡
Ico-Pem	19.62 $\pm$ 1.73	20.12 $\pm$ 2.12†,‡
Ico + Pem	21.75 $\pm$ 0.90	21.07 $\pm$ 1.08†,‡

$P > 0.05$ versus. †Before treatment within-groups and ‡After treatment inter-groups. Ico, icotinib; Ico-Pem, sequential Ico followed by Pemetrexed; Ico + Pem, concurrent Ico combined with Pem; Pem-Ico, sequential Pem followed by Ico; SD, standard deviation

Influence of combined treatment with icotinib and pemetrexed on proliferation and apoptosis rates

There was a significant decrease in the Ki-67 score and an increase in the caspase-3 score in the five drug treated groups compared to the control (56.67 $\pm$ 4.51%, 9.62 $\pm$ 1.39%; $P < 0.01$). The Ki-67 score was lower and the caspase-3 score was higher in the Pem-Ico (13.73 $\pm$ 2.44%, 41.20 $\pm$ 3.14%), Ico + Pem (15.37 $\pm$ 3.11%, 37.83 $\pm$ 3.35%), Ico (34.83 $\pm$ 6.49%, 22.08 $\pm$ 3.01%), and Ico-Pem groups (34.30 $\pm$ 5.90%, 26.72 $\pm$ 2.32%), than in the Pem group (47.13 $\pm$ 3.28%, 13.25 $\pm$ 1.79%) ($P < 0.01$). The Ki-67 scores of the Pem-Ico and Ico + Pem groups were significantly lower than those of the Ico and Ico-Pem groups; by contrast, the caspase-3 scores of the Pem-Ico and Ico + Pem groups were significantly higher than those of the Ico and Ico-Pem groups ($P < 0.01$). No significant differences were identified between the Pem-Ico and Ico + Pem groups or the Ico and Ico-Pem groups. These results showed additive anti-proliferative and proapoptotic activity in the Pem-Ico and Ico + Pem groups (Fig 4).

Effect on regulation of TS, and phosphorylated EGFR, AKT, and MAPK after combined treatment with icotinib and pemetrexed

By Western blotting we found that both icotinib and pemetrexed reduced TS expression, whereas a further reduction was observed in the Pem-Ico and Ico + Pem groups ($P < 0.05$). A decrease in phosphorylation of EGFR, AKT and MAPK proteins was detected among icotinib-containing treatments, with the most significant reductions in the Pem-Ico and Ico + Pem groups ($P < 0.05$). However, there were no significant differences in TS, phospho-EGFR, phospho-AKT, and phospho-MAPK expression levels between the Ico and Ico-Pem groups. In the Pem group, EGFR phosphorylation was slightly enhanced and AKT phosphorylation was slightly inhibited, while MAPK phosphorylation was not affected. These results suggested that the mode of Pem-Ico and Ico + Pem treatments dramatically enhanced the inhibition of TS and phosphorylation of the EGFR signaling pathways (Fig 5).

Discussion

In this study, we established *EGFR*-mutant lung adenocarcinoma cell line HCC827 xenograft models and explored the efficacy of different schedules of pemetrexed and icotinib treatment in xenografts. The best anti-tumor effect was observed in the sequential pemetrexed followed by icotinib group, followed by the concurrent icotinib combined with pemetrexed group; both of these groups were superior to single treatment with icotinib or pemetrexed. However, sequential icotinib followed by pemetrexed did not show any additive effect. These results suggest that administering icotinib concurrent with or after pemetrexed might exert a better effect than using icotinib alone in NSCLC patients with activating *EGFR* mutations.

An important clinical issue is retarding TKI resistance to further increase survival benefits in advanced NSCLC patients with activating *EGFR* mutations. Because NSCLC is a kind of heterogeneous disease, combination treatment with different mechanisms of anti-tumor drugs might further improve outcomes and play a role in preventing drug resistance.[26] A preclinical study reported that acquired gefitinib resistance was prevented when pemetrexed was administered before or together with gefitinib.[27] Recent findings from two phase II clinical trials suggest a potential benefit from the combination of EGFR-TKIs and pemetrexed in *EGFR*-mutant patients.[17,28] Yoshimura *et al.* reported that the sequential administration of gefitinib following pemetrexed obtained a high overall response rate (84.6%) and long median PFS (18 months), with acceptable toxicity.[28] Another phase II JMIT study conducted in
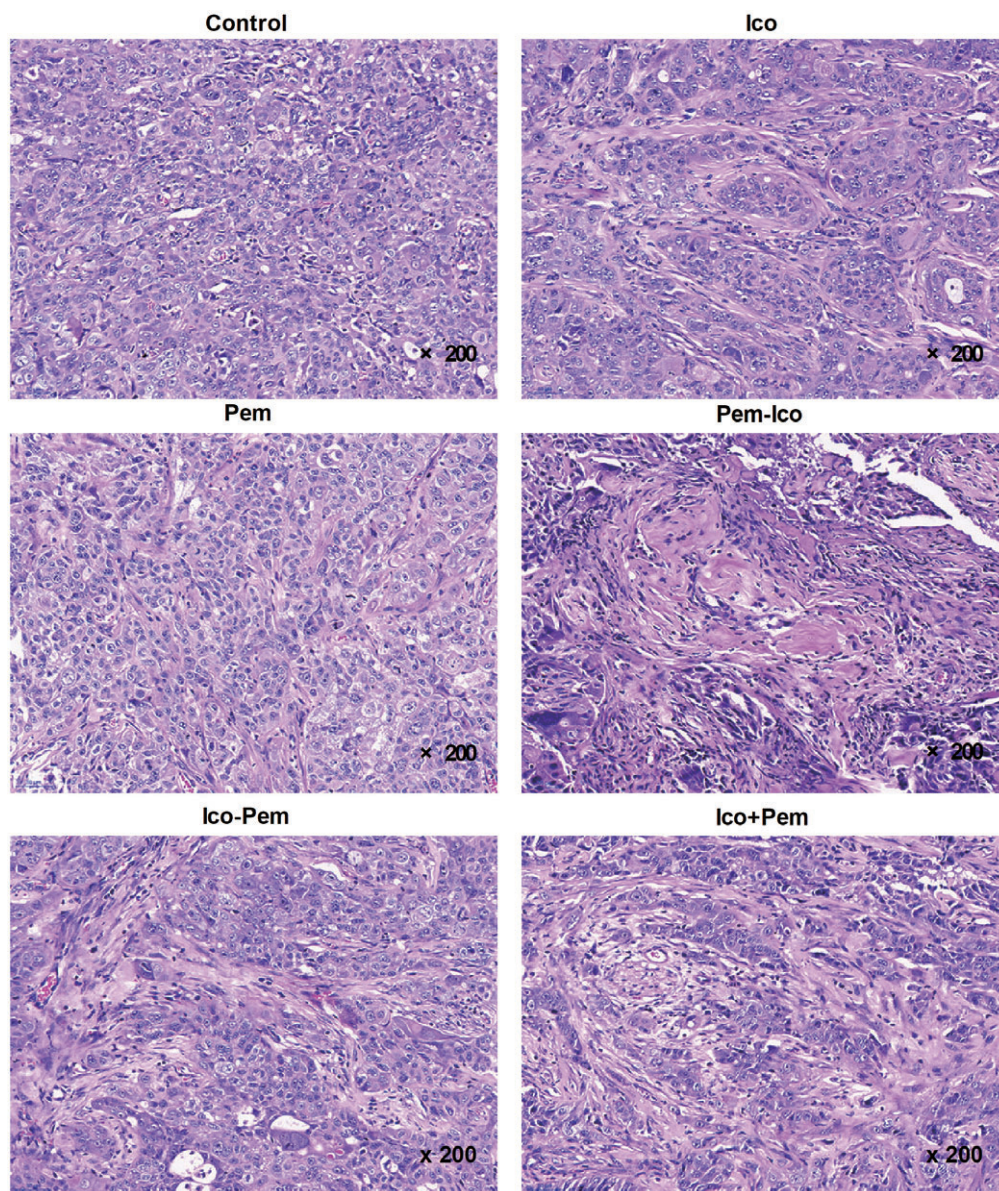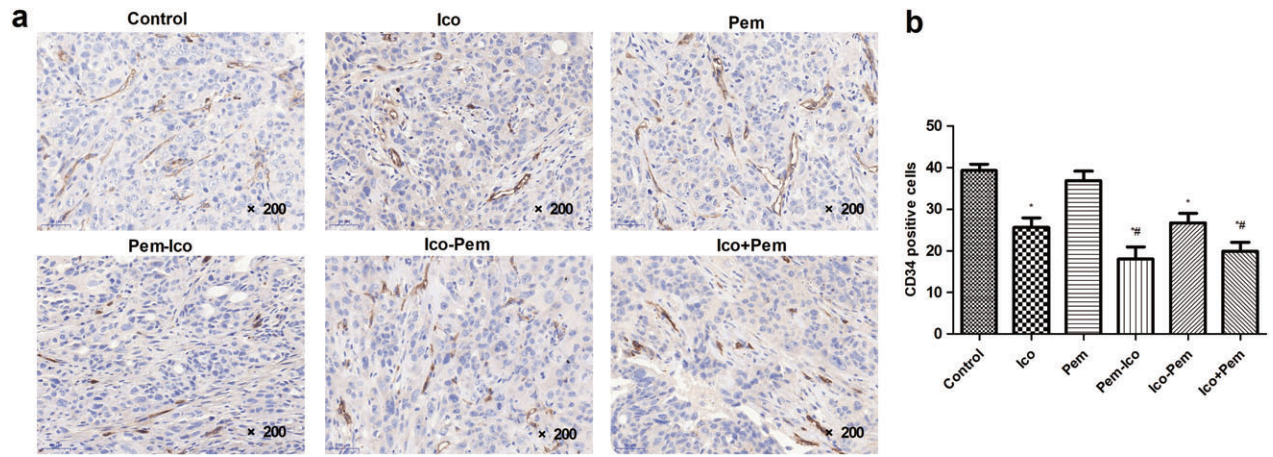
Figure 2 Representative hematoxylin and eosin staining results in tumor xenograft tissues. Groups: control; Ico, icotinib; Ico-Pem, sequential Ico followed by Pem; Ico + Pem, concurrent Ico and Pem; Pem, pemetrexed; Pem-Ico, sequential Pem followed by Ico.

East Asian patients with nonsquamous *EGFR*-mutant NSCLC demonstrated that the concurrent combination of gefitinib and pemetrexed led to a significant improvement of nearly five months in PFS compared to gefitinib alone (hazard ratio 0.68, 95% confidence interval 0.48–0.96; $P = 0.029$).[17] Supporting these results, our data indicate that both the mode of sequential pemetrexed followed by icotinib and concurrent combined icotinib and pemetrexed for the treatment of *EGFR*-mutant lung adenocarcinoma shows promising anti-tumor effects in vivo.

Angiogenesis plays an important role in cancer cell proliferation, invasion, and tumor metastasis. The MVD,

reflecting angiogenesis, is an independent factor of lung cancer prognosis.[29] EGFR-TKIs have proven to have the potential ability to reduce tumor MVD.[30,31] The anti-angiogenic effect of EGFR-TKIs could partially be mediated by blocking epidermal growth factor-induced neovascularization, suggesting that downregulation of EGFR signaling is directly related to the inhibition of angiogenesis.[32] In this study, CD34, as marker of vascular endothelial cells, reflected the status of tumor tissue MVD and was quantitatively analyzed. Tumor xenograft MVD in the Pem-Ico and Ico + Pem groups was dramatically reduced compared to those of the other three treatment

Figure 3 Microvessel density was assessed by immunohistochemical staining for CD34 (stained in brown) in tumor xenograft tissues after the administration of different treatments (*n* = 6 mice/group). Groups: control; Ico, icotinib; Ico-Pem, sequential Ico followed by Pem; Ico + Pem, concurrent Ico and Pem; Pem, pemetrexed; Pem-Ico, sequential Pem followed by Ico. (**a**) Representative immunohistochemical staining results of CD34. (**b**) Microvessel density assessed by CD34 positive cells. The numbers of CD34 positive cells are shown as a histogram: columns, mean ± standard deviation (SD, *n* = 6 mice/group). *P* < 0.01 versus *control and Pem, # Ico and Ico-Pem.
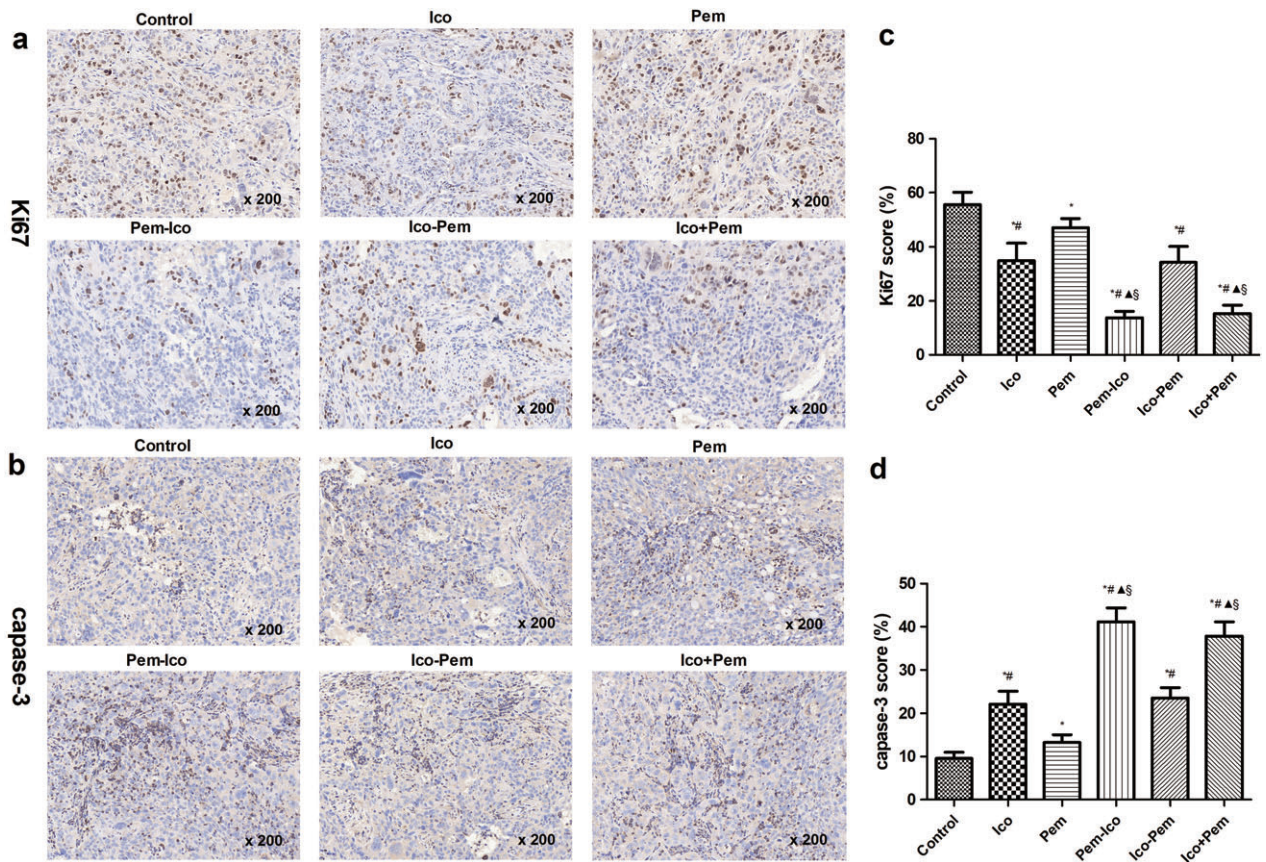
Figure 4 Immunohistochemical analysis of Ki-67 and caspase-3 in tumor xenograft tissues after the administration of different treatments (*n* = 6 mice/group). Groups: control; Ico, icotinib; Ico-Pem, sequential Ico followed by Pem; Ico + Pem, concurrent Ico and Pem; Pem, pemetrexed; Pem-Ico, sequential Pem followed by Ico. Representative immunohistochemical staining results of (**a**) Ki-67 (stained in brown) and (**b**) caspase-3 (stained in brown). (**c**) Proliferation rate assessed by Ki-67 score. (**d**) Apoptosis rate assessed by caspase-3 score. Ki-67 score and caspase-3 score shown as a histogram: columns, mean ± standard deviation. *P* < 0.05 versus *control, #Pem, ▲Ico, §Ico-Pem.
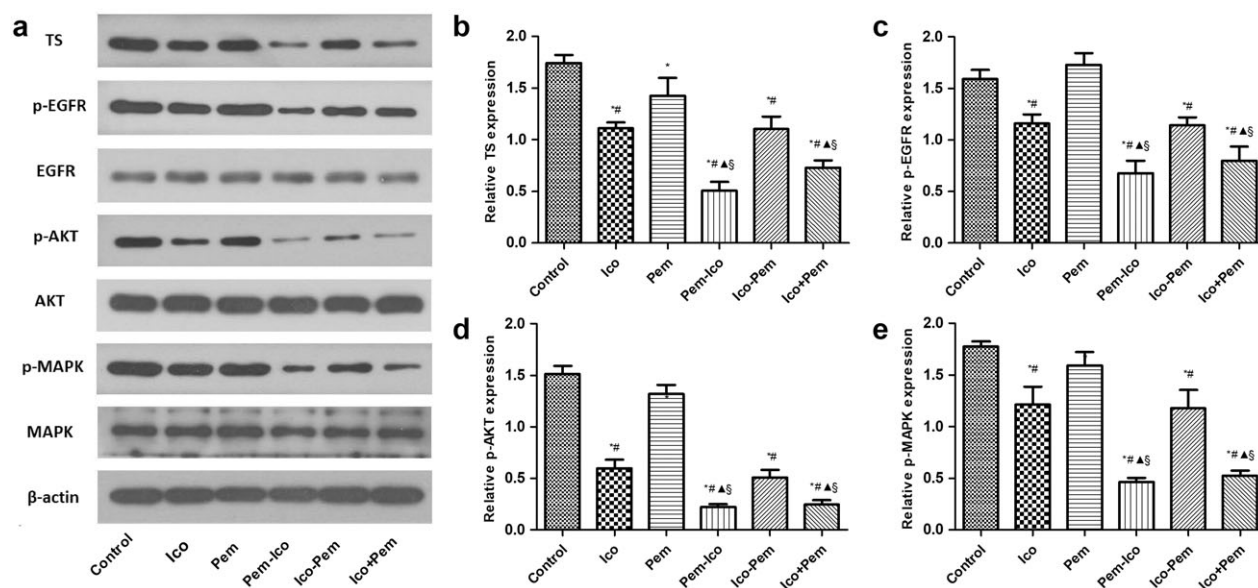
Figure 5 Expression of thymidylate synthase (TS) and related EGFR signaling pathway proteins in tumor xenografts after the administration of different treatments (n = 6 mice/group). Groups: control; Ico, icotinib; Ico-Pem, sequential Ico followed by Pem; Ico + Pem, concurrent Ico and Pem; Pem, pemetrexed; Pem-Ico, sequential Pem followed by Ico. (**a**) The effects of different combinations of Ico and Pem on TS expression and EGFR, AKT, and MAPK phosphorylation in tumor tissues was detected by Western blotting. The relative (**b**) TS (**c**) phospho-EGFR, (**d**) phospho-AKT, and (**e**) phospho-MAPK expression levels. Data are shown as the mean ± standard deviation of triplicate measurements. $P < 0.05$ versus *control, #Pem, ▲Ico, §Ico-Pem.

groups. The additive anti-angiogenesis effect was observed in the Pem-Ico and Ico + Pem groups but not in the Ico-Pem group; these results may relate to differences in EGFR signaling inhibition among the groups, which was also investigated.

The essential feature of malignant tumor development is the process of unlimited proliferation and apoptosis resistance of abnormal cells. Ki-67 is a typical protein marker for cell proliferation activity, and is positively expressed in the proliferative cell nucleus.[33] Caspase-3 is one of the key molecules of the apoptosis pathway, and its activation is a sign of apoptosis entering the irreversible phase.[34] In this study, the proliferation and apoptosis of tumor cells were reflected by Ki-67 and caspase-3 expression, respectively. The proliferation rate was significantly decreased and the apoptosis rate significantly increased in the Pem-Ico and Ico + Pem groups when compared to the other three drug treatment groups (Ico, Pem, and Ico-Pem groups). Moreover, the fibrous tissue increased and tumor cells decreased dramatically in the Pem-Ico and Ico + Pem groups. The proliferation and apoptosis rates in the Ico-Pem and Ico groups were not significantly different, which suggests that sequential icotinib followed by pemetrexed had no obvious advantage over icotinib alone for inhibiting the proliferation or promoting the apoptosis of tumor cells.

As a key enzyme in DNA synthesis, TS is one of the main targets of pemetrexed. The negative correlation between TS expression and the efficacy of pemetrexed has been reported in both in vitro and clinical studies.[35,36] In the present study, icotinib treatment markedly reduced TS expression, and additional reductions were observed in the Pem-Ico and Ico + Pem groups. Similar to a previous in vitro study by La Monica *et al.*, our findings also indicate that the downregulation of TS by icotinib increased the cytotoxicity of pemetrexed for the treatment of *EGFR*-mutant lung adenocarcinoma xenografts when icotinib was administered concurrent with or after pemetrexed.[27] However, compared to icotinib alone, the sequential combination of icotinib followed by pemetrexed did not further reduce TS expression. In addition, the inhibition of EGFR, AKT and MAPK phosphorylation was enhanced when icotinib was administered concurrent with or after pemetrexed, which is consistent with the concept that EGFR signaling pathways are more susceptible to inhibition by TKIs because pemetrexed increases EGFR phosphorylation.[37] The RAS/MAPK/ERK-dependent pathway is one of the major *EGFR* downstream signaling pathways and induces the elevation of cyclin D1 levels, while the downregulation of cyclin D1 leads to E2F-1 inhibition.[38] The additional decreased TS levels found in our study after the administration of concurrent EGFR-TKI and pemetrexed may have been the result of enhanced downregulation of E2F-1 expression.[37] It is worth noting that the inhibitory effect on EGFR, AKT, and MAPK phosphorylation in the

Ico-Pem group was significantly weaker than in the Pem-Ico and Ico + Pem groups, but not the Ico group. Hence, we speculate that the sequential treatment associated inhibition of TS expression might be related to the downregulated level of the RAS/MAPK/ERK pathway in each combined icotinib and pemetrexed group, respectively. The inhibition of TS expression could also be explained by the interaction of icotinib and pemetrexed in vivo. Further work is needed to clarify the relationship between TS expression and cyclin D1 in *EGFR*-mutant NSCLC cells.

Both modes of sequential pemetrexed followed by icotinib and concurrent combinations of icotinib and pemetrexed showed additive anti-tumor activity by reducing angiogenesis, enhancing anti-proliferative and proapoptotic effects, and the inhibition of TS expression and EGFR downstream signaling pathways. No antagonism between pemetrexed and icotinib was observed in the group administered sequential icotinib followed by pemetrexed, which did not match in vitro results, possibly because of the different durations of treatment and the changing biological characteristics of the tumor cells resulting from the complex microenvironment. Our study provides evidence for conducting clinical trials using combined icotinib and pemetrexed in patients with *EGFR*-mutant lung adenocarcinoma.

Acknowledgments

Disclosure

No authors report any conflict of interest.

REFERENCES

1 Siegel RL, Miller KD, Jemal A. Cancer statistics, 2016. *CA Cancer J Clin* 2016; **66**: 7–30.

2 Kumarakulasinghe NB, van Zanwijk N, Soo RA. Molecular targeted therapy in the treatment of advanced stage non-small cell lung cancer (NSCLC). *Respirology* 2015; **20**: 370–8. (Published erratum appears in Respirology 2016;21:567).

3 Schiller JH, Harrington D, Belani CP *et al.* Comparison of four chemotherapy regimens for advanced non-small-cell lung cancer. *N Engl J Med* 2002; **346**: 92–8.

4 Mok TS, Wu YL, Thongprasert S *et al.* Gefitinib or carboplatin-paclitaxel in pulmonary adenocarcinoma. *N Engl J Med* 2009; **361**: 947–57.

5 Kwak EL, Bang YJ, Camidge DR *et al.* Anaplastic lymphoma kinase inhibition in non-small-cell lung cancer. *N Engl J Med* 2010; **363**: 1693–703. (Published erratum appears in N Engl J Med 2011; 364: 588).

6 Zhou C, Wu YL, Chen G *et al.* Erlotinib versus chemotherapy as first-line treatment for patients with advanced EGFR mutation-positive non-small-cell lung cancer (OPTIMAL, CTONG-0802): A multicentre, open-label, randomised, phase 3 study. *Lancet Oncol* 2011; **12**: 735–42.

7 Jackman D, Pao W, Riely GJ *et al.* Clinical definition of acquired resistance to epidermal growth factor receptor tyrosine kinase inhibitors in non-small-cell lung cancer. *J Clin Oncol* 2010; **28**: 357–60.

8 Giaccone G, Herbst RS, Manegold C *et al.* Gefitinib in combination with gemcitabine and cisplatin in advanced non-small-cell lung cancer: A phase III trial--INTACT 1. *J Clin Oncol* 2004; **22**: 777–84.

9 Herbst RS, Giaccone G, Schiller JH *et al.* Gefitinib in combination with paclitaxel and carboplatin in advanced non-small-cell lung cancer: A phase III trial--INTACT 2. *J Clin Oncol* 2004; **22**: 785–94.

10 Herbst RS, Prager D, Hermann R, Fehrenbacher L *et al.* TRIBUTE: A phase III trial of erlotinib hydrochloride (OSI-774) combined with carboplatin and paclitaxel chemotherapy in advanced non-small-cell lung cancer. *J Clin Oncol* 2005; **23**: 5892–9.

11 Gatzemeier U, Pluzanska A, Szczesna A *et al.* Phase III study of erlotinib in combination with cisplatin and gemcitabine in advanced non-small-cell lung cancer: The Tarceva Lung Cancer Investigation Trial. *J Clin Oncol* 2007; **25**: 1545–52.

12 Wu YL, Lee JS, Thongprasert S *et al.* Intercalated combination of chemotherapy and erlotinib for patients with advanced stage non-small-cell lung cancer (FASTACT-2): A randomised, double-blind trial. *Lancet Oncol* 2013; **14**: 777–86.

13 Chattopadhyay S, Moran RG, Goldman ID. Pemetrexed: Biochemical and cellular pharmacology, mechanisms, and clinical applications. *Mol Cancer Ther* 2007; **6**: 404–17.

14 Paz-Ares LG, Zimmermann A, Ciuleanu T *et al.* Meta-analysis examining impact of age on overall survival with pemetrexed for the treatment of advanced non-squamous non-small cell lung cancer. *Lung Cancer* 2017; **104**: 45–51.

15 Li T, Ling YH, Goldman ID, Perez-Soler R. Schedule-dependent cytotoxic synergism of pemetrexed and erlotinib in human non-small cell lung cancer cells. *Clin Cancer Res* 2007; **13**: 3413–22.

16 Feng X, Zhang Y, Li T, Li Y. Sequentially administered of pemetrexed with icotinib/erlotinib in lung adenocarcinoma cell lines in vitro. *Oncotarget* 2017; **8**: 114292–9.

17 Cheng Y, Murakami H, Yang PC *et al.* Randomized phase II trial of gefitinib with and without pemetrexed as first-line therapy in patients with advanced nonsquamous non-small-cell lung cancer with activating epidermal growth factor receptor mutations. *J Clin Oncol* 2016; **34**: 3258–66.

18 Shi Y, Zhang L, Liu X *et al.* Icotinib versus gefitinib in previously treated advanced non-small-cell lung cancer

(ICOGEN): A randomised, double-blind phase 3 non-inferiority trial. *Lancet Oncol* 2013; **14**: 953–61.

19 Hall RD, Le TM, Haggstrom DE, Gentzler RD. Angiogenesis inhibition as a therapeutic strategy in non-small cell lung cancer (NSCLC). *Transl Lung Cancer Res* 2015; **4**: 515–23.

20 Hirata A, Ogawa S, Kometani T *et al.* ZD1839 (Iressa) induces antiangiogenic effects through inhibition of epidermal growth factor receptor tyrosine kinase. *Cancer Res* 2002; **62**: 2554–60.

21 Cheng H, An SJ, Zhang XC *et al.* In vitro sequence-dependent synergism between paclitaxel and gefitinib in human lung cancer cell lines. *Cancer Chemother Pharmacol* 2011; **67**: 637–46.

22 Erdem O, Erdem M, Erdem A, Memis L, Akyol G. Expression of vascular endothelial growth factor and assessment of microvascular density with CD 34 and endoglin in proliferative endometrium, endometrial hyperplasia, and endometrial carcinoma. *Int J Gynecol Cancer* 2007; **17**: 1327–32.

23 Tan F, Shen X, Wang D *et al.* Icotinib (BPI-2009H), a novel EGFR tyrosine kinase inhibitor, displays potent efficacy in preclinical studies. *Lung Cancer* 2012; **76**: 177–82.

24 Morfouace M, Shelat A, Jacus M *et al.* Pemetrexed and gemcitabine as combination therapy for the treatment of Group3 medulloblastoma. *Cancer Cell* 2014; **25**: 516–29.

25 Kendrew J, Odedra R, Logié A *et al.* Anti-tumour and anti-vascular effects of cediranib (AZD2171) alone and in combination with other anti-tumour therapies. *Cancer Chemother Pharmacol* 2013; **71**: 1021–32.

26 Bai H, Wang Z, Chen K *et al.* Influence of chemotherapy on EGFR mutation status among patients with non-small-cell lung cancer. *J Clin Oncol* 2012; **30**: 3077–83.

27 La Monica S, Madeddu D, Tiseo M *et al.* Combination of gefitinib and pemetrexed prevents the acquisition of TKI resistance in NSCLC cell lines carrying EGFR-activating mutation. *J Thorac Oncol* 2016; **11**: 1051–63.

28 Yoshimura N, Kudoh S, Mitsuoka S *et al.* Phase II study of a combination regimen of gefitinib and pemetrexed as first-line treatment in patients with advanced non-small cell lung cancer harboring a sensitive EGFR mutation. *Lung Cancer* 2015; **90**: 65–70.

29 Meert AP, Paesmans M, Martin B *et al.* The role of microvessel density on the survival of patients with lung cancer: A systematic review of the literature with meta-analysis. *Br J Cancer* 2002; **87**: 694–701.

30 Oh HY, Kwon SM, Kim SI, Jae YW, Hong SJ. Antiangiogenic effect of ZD1839 against murine renal cell carcinoma (RENCA) in an orthotopic mouse model. *Urol Int* 2005; **75**: 159–66.

31 Hara F, Aoe M, Doihara H *et al.* Antitumor effect of gefitinib ('Iressa') on esophageal squamous cell carcinoma cell lines in vitro and in vivo. *Cancer Lett* 2005; **226**: 37–47.

32 Ono M, Kuwano M. Molecular mechanisms of epidermal growth factor receptor (EGFR) activation and response to gefitinib and other EGFR-targeting drugs. *Clin Cancer Res* 2006; **12**: 7242–51.

33 Berghoff AS, Ilhan-Mutlu A, Dinhof C *et al.* Differential role of angiogenesis and tumour cell proliferation in brain metastases according to primary tumour type: Analysis of 639 cases. *Neuropathol Appl Neurobiol* 2015; **41**: e41–55.

34 Lim YJ, Jeon SR, Koh JM, Wu HG. Tumor growth suppression and enhanced radioresponse by an exogenous epidermal growth factor in mouse xenograft models with A431 cells. *Cancer Res Treat* 2015; **47**: 921–30.

35 Giovannetti E, Mey V, Nannizzi S *et al.* Cellular and pharmacogenetics foundation of synergistic interaction of pemetrexed and gemcitabine in human non-small-cell lung cancer cells. *Mol Pharmacol* 2005; **68**: 110–8.

36 Chen CY, Chang YL, Shih JY *et al.* Thymidylate synthase and dihydrofolate reductase expression in non-small cell lung carcinoma: The association with treatment efficacy of pemetrexed. *Lung Cancer* 2011; **74**: 132–8.

37 Giovannetti E, Lemos C, Tekle C *et al.* Molecular mechanisms underlying the synergistic interaction of erlotinib, an epidermal growth factor receptor tyrosine kinase inhibitor, with the multitargeted antifolate pemetrexed in non-small-cell lung cancer cells. *Mol Pharmacol* 2008; **73**: 1290–300.

38 Kobayashi S, Shimamura T, Monti S *et al.* Transcriptional profiling identifies cyclin D1 as a critical downstream effector of mutant epidermal growth factor receptor signaling. *Cancer Res* 2006; **66**: 11389–98.